Passivity considerations in robust spectral-based controllers for wave energy converters

Demián García-Violini[1*], Mahdiyeh Farajvand[2†], Christian Windt[3‡], Valerio Grazioso[4†],and John V. Ringwood[5†]
[*]Departamento de Ciencia y Tecnología, Universidad Nacional de Quilmes, R. S. Peña 352, Bernal B1876, Argentina.
[†]Centre for Ocean Energy Research, Maynooth University, W23 F2K8, Co. Kildare, Ireland.
[‡]Leichtweiß-Institute for Hydraulic Engineering and Water Resources, Beethovenstr. 51a, 38106, Braunschweig, Germany.
[1]ddgv83@gmail.com (corresponding author), [4]c.windt@tu-braunschweig.de,
[2]mahdiyeh.farajvand.2021@mumail.ie; {[4]valerio.grazioso; [5]john.ringwood}@mu.ie

***Abstract*—Recent developments in wave energy converter (WEC) control include robust control strategies, which admit a level of uncertainty in the model description. Then, for the application of such control methods, some knowledge of the uncertainty bounds is initially required. As recently shown in the literature, some approaches for uncertainty quantification can lead to scenarios where, due to uncertainty quantification, the passivity of the WEC model is not guaranteed and, consequently, the optimisation required to capture most of the available energy cannot be successfully performed. Such approaches can generate significant performance losses. Thus, in this study, a passivisation methodology to extend the applicability of spectral control approaches is presented. The benefit of the presented approach, relative to previous results, is shown with an application case.**

***Index Terms*—Wave energy; Energy maximising control; WEC systems; Spectral Methods; Passivisation**

I. Introduction

The operation of wave energy converters (WECs) in realistic environments involves dynamics of the different conversion stages and complex fluid-structure interactions, posing considerable uncertainty in device modelling. In particular, the fact that, in controlled WECs, the dynamic range of motion is considerably exaggerated, adds a significant uncertainty source to the model description, mainly when linearity assumptions, as generally used in the WEC field, are challenged. Thus, efficiently handling of WEC model uncertainty, due to non-linearity or other unmodelled dynamics, represents a key factor in the development of effective control strategies. Conversely, neglecting such system uncertainties negatively impacts on the resulting control performance.

Sensitivity and robustness issues, due to a number of different hydrodynamical sources, have been recently reported in the literature for control of WEC systems [1]–[5], with important consequences [6]. Robust energy maximising control strategies, based on spectral methods and moment-matching theory, are presented in [1] and [2], respectively, assuming uncertainty in the model. Using computational fluid dynamics (CFD), the estimation of numerical uncertainty for a point absorber with a passive controller is studied in [4]. Furthermore, in [3], using the robust control strategy presented in [1], a complete study of uncertainty estimation, is presented, particularly focusing on passivity issues related to uncertainty quantification. Similarly to [4], CFD-based simulations are also used in [3] for uncertainty boundary estimation in the application case. The interested reader is referred to [5] for a further study related to uncertainty analysis.

For energy maximisation control problems, uncertainty or non-linearity in the device model can occur, and even be magnified, as the device motion is exaggerated by control action. Thus, a clear modelling paradox [7] is established between control objectives and models used for control design. In addition, in terms of model uncertainty, the selection of a suitable nominal model (NM) will also positively impact on the resulting control performance [3]. To effectively articulate uncertainty and non-linearities, CFD represents a fully non-linear hydrodynamic description of WECs, based on solving the Navier-Stokes equations, for the analysis of fluid behaviour.

Within this context, as shown in [3], where the results presented in [1] are implemented, with an added uncertainty quantification study, critical passivity issues can arise from the analysis and estimation of uncertainty sets in WEC systems. However, even when the uncertainty boundaries are determined from experimental or high fidelity simulations, these boundaries can contain cases where passivity is not fully satisfied. Thus, in [3], to achieve the implementation of spectral-based control methodologies, the spectral components that violate passivity requirements are removed. However, this spectral-component suppression negatively impacts on the resulting performance, since the power sources related to those neglected spectral components do not contribute to the final performance.

Considering the passivity issues related to uncertainty estimation procedures, a passivisation methodology is presented in this study. Furthermore, considering that robust methodologies based on spectral/pseudospectral and moment-matching methods [1], [2] can lead to predominantly conservative scenarios, a practical conservatism

relaxation is also employed to provide a degree of passivisation design freedom. Thus, this study aims to extend the applicability of existing energy maximising control strategies in those cases where, due to the inexact estimation of uncertainty region, there are obstacles for the application of the control methods. In addition, based on WEC motion data generated using CDF-based simulations, the presented passivisation procedure is shown with an application case, highlighting the benefit of the presented methodology, in contrast with existing results available in the literature [3]. From a general perspective, the presented passivisation method can deal with those spectral components that would be excluded with standard approaches [1], [2].

The remainder of this paper is organised as follows. The basics of WEC dynamics, and its corresponding objective function, in terms of energy maximisation, is introduced in Section II. The basics of spectral/pseudospectral methods for the nominal and robust cases are briefly recalled in Sections III-A and III-B, respectively. The main core of the proposed methodology, with a discussion on the selection of the NM from an uncertainty perspective, is presented in Section IV. The application case is shown in Section V. Finally, conclusions on the overall application of the proposed methodology are provided in Section VI.

II. WEC model and Objective Function

A. WEC Model

WEC models, considered for the control problems, are typically based on a linear hydrodynamic formulation, known as Cummins equation. Under the assumption of an inviscid fluid and irrotational and incompressible incident flow, the equation of motion for a WEC, in terms of Cummins equation [8], can be expressed as:

$$(M + m_\infty)\ddot{x}_p(t) + \dot{x}_p(t) * h_r(t) + s_h x_p(t) = f_{ex}(t) + f_u(t), \quad (1)$$

where $*$ denotes the convolution operator, $x_p(t)$, $\dot{x}_p(t) = v(t)$ and $\ddot{x}_p(t)$ are the WEC position, velocity, and acceleration, respectively; M is the mass of the oscillating body, and m_∞ the added mass at infinite frequency; $h_r(t)$ is the radiation force impulse response; and s_h is hydrodynamic stiffness, related to the buoyancy force. Additionally, in Eq. (1), $f_{ex}(t)$ is the wave excitation force, produced by the action of incoming waves, and $f_u(t)$ represents the control force applied through the power take-off (PTO) system. The interested reader is referred to [9] for a comprehensive description of WEC dynamics.

B. Energy Absorption: Objective Function

The useful absorbed energy over the time interval $\begin{bmatrix}0 & T\end{bmatrix}$, $T > 0$ can be calculated as follows:

$$J \equiv E = -\int_0^T P dt = -\int_0^T v^\intercal(t) f_u(t) dt. \quad (2)$$

where E represents the absorbed energy, P the instantaneous power, and $f_u(t)$ and $v(t) = \dot{x}_p(t)$ are defined in Eq. (1). From a general perspective, the control problem consists of obtaining the PTO control force $f_u(t)$ that maximises the objective function J, defined in Eq. (2), subject to the equation of motion, in Eq. (1), and a set of physical constraints $\mathcal{C}$.

III. Energy Maximising Control of WECs with Spectral/Pseudospectral Methods

In this section, the basics of spectral/pseudospectral methods are briefly discussed. The interested reader is referred to [1] and [10] for a comprehensive discussion on this family of energy maximising control methods. Spectral/speudospectral methods are utilised to discretise, in the spectral domain, the energy maximising problem stated in Eq. (2). Thus, these methods approximate the states, control variables, and inputs, in an N-dimensional vector space, with a linear combination of orthogonal basis functions $\Phi(t)$. Then, using spectral/speudospectral methods, the nominal WEC force-to-velocity mapping, G_o, is described as an algebraic relationship, instead of the integro-differential description stated in Eq. (1). Furthermore, the basis functions are chosen such that the force-to-velocity mapping, G_o, is defined as a block diagonal matrix comprised with the real and imaginary parts of the force-to-velocity frequency response [10].

A. Nominal Case

The application of spectral/pseudospectral approximations to the objective function J results in:

$$J \approx J_N = \int_0^T \hat{\mathrm{u}}^\intercal \Phi^\intercal(t) \Phi(t) \hat{\mathrm{v}} = -\frac{T}{2} \hat{\mathrm{u}}^\intercal \hat{\mathrm{v}}, \quad (3)$$

where the vectors $\hat{\mathrm{u}}^\intercal$ and $\hat{\mathrm{v}}$ represent the spectrally discretised versions of the control input and device velocity, respectively, i.e. $v(t) \approx \Phi(t)\hat{\mathrm{v}}$ and $f_u(t) \approx \Phi(t)\hat{\mathrm{u}}$. Then, the following algebraic equality is obtained:

$$J_N = -\frac{T}{2} \hat{\mathrm{u}}^\intercal G_o (\hat{\mathrm{u}} + \hat{\mathrm{e}}), \quad (4)$$

with $\hat{\mathrm{e}}$ the spectral discretisation of $f_{ex}(t)$ and $\hat{\mathrm{v}} = G_o(\hat{\mathrm{u}} + \hat{\mathrm{e}})$. Thus, Eq. (4) is a quadratic function in the control variable $\hat{\mathrm{u}}$. In order to guarantee the existence of a unique maximum value for the objective function of the WEC, the system must be passive, i.e. its transfer function should be positive real [11]. When the optimal solution of the problem expressed in Eq. (4) is guaranteed, the optimal control problem can be restated as:

$$\hat{\mathrm{u}}_o^\star \leftarrow \begin{array}{rl} \max\limits_{\forall \hat{\mathrm{u}}_o \in \mathbb{R}^N} & J_N \\ \text{s.t.} & \mathcal{C} \end{array}, \quad (5)$$

where $\hat{\mathrm{u}}_o^\star$ denotes the optimal solution of the optimisation problem and $\mathcal{C}$ a set of constraints, generally defined in terms of motion or actuator limits.

B. Robust Case

The spectral/pseudospectral methods discussed in Section III-A are based on a precise description of the system. To proceed with the robust approach [1], a *real* system is described using the NM and an uncertainty set. The real system can be defined using an additive perturbation, Δ_a, which takes the following form:

$$\Delta_a = \bigoplus_{k=1}^{N/2} \begin{bmatrix} \delta_k^{\mathcal{R}} & \delta_k^{\mathcal{I}} \\ -\delta_k^{\mathcal{I}} & \delta_k^{\mathcal{R}} \end{bmatrix}, \tag{6}$$

where $\Delta_a \in \mathbb{R}^n$ is a block diagonal matrix and the symbol $\bigoplus$ denotes the direct sum of n matrices, i.e. $\bigoplus_{i=1}^{n} A_i = diag\{A_1,\ A_2,\ \cdots, A_n\}$. Then, objective function J_N, defined for the nominal case in Eq. (4), is redefined for the robust case as:

$$J_N = -\frac{T}{2}\hat{\mathrm{u}}^{\intercal}\left(G_o + \Delta_a\right)\left(\hat{\mathrm{u}} + \hat{\mathrm{e}}\right). \tag{7}$$

Particularly, for the Fourier basis,

$$g(j\omega_k) = g_o(j\omega_k) + \delta_k \Leftrightarrow \delta_k = g(j\omega_k) - g_o(j\omega_k),$$

where $\delta_k \in \mathbb{C}$ represents the uncertainty level at the frequency ω_k with $\delta_k^{\mathcal{R}} = \mathbb{R}e\{\delta_k\}$ and $\delta_k^{\mathcal{I}} = \mathbb{I}m\{\delta_k\}$.

Using the feasibility condition defined in [1] (in Eq. (16)), and defining the best worst-case performance (WCP) solution as the input that minimises the performance degradation when the system under study is affected by a bounded uncertainty set Δ_a, the robust control problem statement can be defined as:

$$\hat{\mathrm{u}}_r^{\star} \leftarrow \begin{array}{ccc} \max & \min & J_N \\ \hat{\mathrm{u}}_r \in \mathbb{R}^N & \Delta_a \in \mathcal{U} & \\ & \text{s.t.} & \mathcal{C} \end{array}. \tag{8}$$

Eq. (8) describes a minimax problem, where $\mathcal{U}$ indicates the set of all possible uncertainties. The problem in Eq. (8), originally presented in [1], can be solved using general purpose optimisation toolboxes for minimax problems. It should be noted that, for the application of the control strategy presented in [1], the passivity of the complete family of models, is assumed, which is indicated in [1] as a feasibility condition. However, when the uncertainty bounds are estimated from experimental (or simulated) data, the passivity condition is not necessarily fulfilled for all the spectral components ω_k, for two reasons. Firstly, due to practical issues, such as numerical errors or non-linear behaviour, the location of some spectral components may violate the passivity of the system. Consequently, due to the obtained experimental data, the nominal description of the model will not satisfy the passivity requirement. Secondly, due to the uncertainty quantification procedure, some boundaries can be, at least partially contained in the left-hand plane (LHP), which generates a passivity violation. Thus, in both cases, the control approach presented in [1] cannot be applied, as discussed in [3].

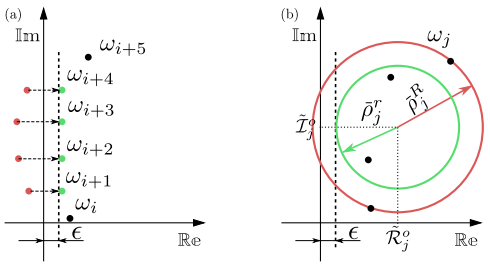

Fig. 1. (a) passivisation of the NM (b) passivisation of the uncertainty set.

IV. Practical issues: Passivisation and NM

As discussed in Section III-B, there are practical issues that can arise from an uncertainty quantification process, and, consequently, critical implementation obstacles are obtained. Within this framework, two potential scenarios are possible. The first scenario is when the obtained *nominal* representation of the WEC system does not fulfil the passivity condition. The second scenario is obtained when the *uncertainty structure*, quantified using the geometrical structures suggested in [1] and [2], does not satisfy the feasibility condition in [1], for at least one (or more) spectral component. To deal with these two scenarios, the proposed methodology is described in Sections IV-A1 and IV-A2, while a brief discussion about practical issues that arise from the NM definition, is provided in Section IV-B, from the perspective of *control-oriented* models and uncertainty quantification.

A. Passivisation Methodology

To overcome the issues articulated in Sections III-B and IV, two main practical considerations are examined in this section. The proposed procedure is essentially described in Figs. 1(a) and (b), where the two situations covered in this study, detailed in Sections IV-A1 and IV-A2, are depicted. It is important to take into account that the presented methodology, must be finally validated using the experimental data. Thus, the proposed method, which indirectly aims to relax the intrinsic conservatism of the aforementioned control strategies [1], [2], requires final validation, based on simulations.

1) NM Rectification: The first situation results when the defined NM is, at least, partially contained in the LHP, as shown in Fig. 1(a), indicated by red dots. In this case, the presented model rectification methodology proposes to shift the spectral components contained in the LHP to the right-half plane (RHP), to fulfil the passivity requirement. Then, for a particular spectral component, this rectification procedure, which essentially redefines the real part of the NM, $\mathcal{R}_o^k$, related to the $k-th$ spectral component, ω_k, can be described by:

$$\tilde{\mathcal{R}}_k^o = \begin{cases} \mathcal{R}_k^o & if \quad \mathcal{R}_k^o > 0 \\ \epsilon & if \quad \mathcal{R}_k^o \leq 0 \end{cases}, \tag{9}$$

which, by way of example, is indicated using the green dots in Fig. 1(a), for $\omega_k \in \{\omega_j\}$ with $j = i+1, \ldots, i+4$. In addition, as indicated for Eq. (9), an infinitesimal margin $0 < \epsilon$, required for numerical reasons in the computation of the control input, is also considered in Eq. (9).

2) Uncertainty Boundaries Correction: The second situation, which, as described before, is obtained when the uncertainty structures are not entirely contained in the RHP, is depicted in Fig. 1(b) for a given spectral component, ω_j, using circular boundaries. It is important to note that the essence of the presented passivisation methodology is described, without loss of generality, in Fig. 1(b), even though a circular boundary case is used in Fig. 1(b). Thus, the presented passivisation methodology aims to rectify those uncertainty areas, which violate the passivity condition, forcing these regions to be fully contained in the RHP, while the uncertainty geometry is preserved. This passivisation procedure can be described, for the circular case, as:

$$\tilde{\mathcal{C}}^k \leftarrow \begin{cases} \tilde{\rho}_k = \bar{\rho}_k & if \quad \bar{\rho}_k > |\tilde{\mathcal{R}}_k^o| \\ \tilde{\rho}_k = \tilde{\mathcal{R}}_k^o - \epsilon & if \quad \bar{\rho}_k \leq |\tilde{\mathcal{R}}_k^o| \end{cases}, \tag{10}$$

where each radius $\bar{\rho}_k$, related to a spectral component ω_k, which does not satisfy the passivity condition for the complete family of models, is corrected, preserving its center and structure, using a radius $\tilde{\rho}_k$. Then, a rectified uncertainty structure $\tilde{\mathcal{C}}_k$, which fully guarantees passivity, is obtained. In Fig. 1(b), by way of example, the passivisation procedure, applied to a circular uncertainty region, defined by the spectral component ω_j and its radius $\bar{\rho}_j^R$, indicated with a red circle, is shown. Thus, the resulting rectified uncertainty region is indicated in Fig. 1(b), using a green circle and a radius $\bar{\rho}_j^r$, where, similarly to Eq. (9), an infinitesimal margin $0 < \epsilon$ has been also considered in Eq. (10).

B. Practical Considerations in the NM Definition

The definition of a suitable *control-oriented* NM represents a key driver for achieving satisfactory performance levels in general control problems. In general parametric model-based robust control strategies, the initial uncertainty reduction is targeted at the definition of the empirical-transfer function estimated (ETFE), used for the computation of the NM. With the aim of reducing the associated uncertainty level, the circles of minimum radius, that contain all experiments for each spectral component, are considered in [3], and also in the application case of this study, in Section V.

V. Application Case

The considered numerical CFD setup, also used in [3], is detailed in Figs. 2(a) and 2(b), where the WEC and tank (side view) dimensions are detailed, respectively. The mass of the WEC system is 43.67 kg. Further details of the numerical setup can be found in [3]. Fully non-linear hydrodynamic simulation of the device is implemented using the open-source CFD toolbox OpenFOAM [12]. The application case is addressed in different stages, as shown in the following.

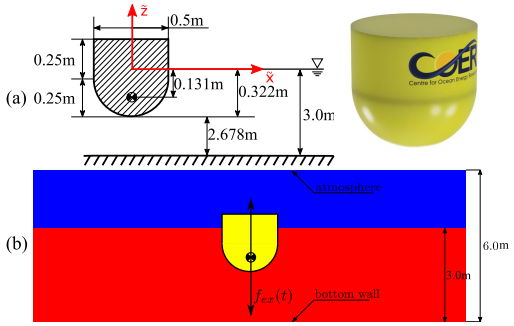

Fig. 2. Schematic of the (a) WEC structure and (b) numerical wave tank (side view).

A. WEC System Characterisation: NM

In a first experimental stage, a description of the WEC system is obtained. Thus, a set of chirp-up experiments, each one indicated in this study using the index i, is performed. It is important to note that, in these tests, the device motion is solely driven by the control force $f_u(t)$; i.e. $f_{ex}(t) = 0$. The amplitude of each control force signal, $f_u^i(t)$, is contained in $A_i \in \{10, 20, 40, 50, 60\}$ N, and a linear frequency variation rate from 1 to 20 $\frac{\text{rad}}{s}$ is used, while, to minimise reflection effects in the numerical wave tank, a 25 s time-length is employed for each experiment. Thus, while each chirp-up control force signal, $f_u^i(t)$, is applied, the corresponding WEC velocity, $v^i(t)$, is measured as the output of the system. Then, the force-to-velocity mapping, required for the controller computation [9], is obtained. Thus, a set of ETFEs is computed as follows:

$$G_i(\omega) = \frac{V^i(\omega)}{F_u^i(\omega)}, \text{ with } \omega \in \Omega \subseteq [1,\ 20], \tag{11}$$

where $V^i(\omega)$ and $F_u^i(\omega)$ denote the Fourier transform of $f_u^i(t)$ and $v^i(t)$, respectively, and Ω the frequency domain.

B. Wave Excitation Force

In the second experimental stage, wave excitation force tests are run in the CFD environment, where the WEC is exposed to irregular incident waves, taken from a JONSWAP spectrum with a significant wave height of $Hs = 0.1$ m, peak period $T_p = 1.94$ s, and steepness parameter $\lambda = 3.3$. This simulation condition represents a scaled version of a realistic operation scenario in the full scale device. To obtain a measure of the wave excitation force, $f_{ex}(t)$, a fixed-body experiment is run [3]. Thus, a Fourier set of basis functions, given by $\Phi(t) = \left[\cos(\omega_1 t)\ \ \sin(\omega_1 t)\ \ \cdots\ \ \cos(\omega_{63} t)\ \ \sin(\omega_{63} t)\right]$, where the frequency vector, $\omega_k = 0.0642k + 2.3446$ with $k = 1, 2, \ldots, 63$, is empirically determined to achieve over a 95% accuracy in the spectral wave excitation force approximation, $\tilde{f}_{ex}(t)$, while keeping a low level of burden.

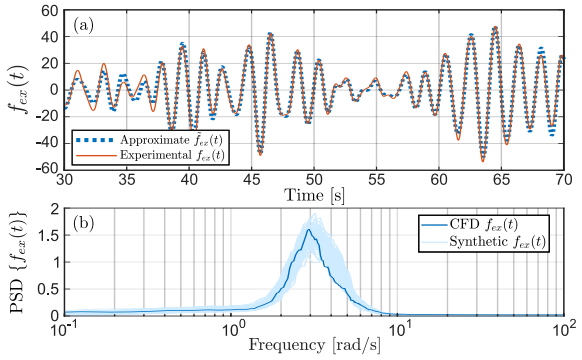

Fig. 3. (a) Experimental and approximated wave excitation force. (b) PSD of the CFD-based and synthetic $f_{ex}(t)$ signals.

The obtained wave excitation force, $f_{ex}(t)$, and its approximation, $\tilde{f}_{ex}(t)$, are shown in Fig. 3(a) using dotted-blue and solid-orange lines, respectively. In addition, the power spectral density (PSD) of $f_{ex}(t)$ is shown in Fig. 3(b), using a deep-blue-solid line. Considering the CFD-based $f_{ex}(t)$, synthetically generated wave excitation force signals are employed to extend the statistical consistency of the results presented in Section V-E. The PSD of synthetically generated wave excitation force signals, are shown using light-blue-solid lines in Fig. 3(b).

C. NM Definition and Uncertainty Quantification

As in [3], the NM, used for the controller computation, is defined with the aim of minimising the uncertainty magnitude. To this end, over the frequency domain, Ω, used to describe the ETFEs defined in Eq. (11), for each single frequency $\omega^\star \in \Omega$ the circle of minimum radius that contains the ETFEs, defined in Eq. (11), is computed. The center of each minimum radius circle, $(\mathcal{R}_k^o, \mathcal{I}_k^o)$, where $k = 1, \ldots, 63$ indicates the particular spectral component, is used to define the NM G_o and, in terms of an additive structure, the uncertainty set $\mathcal{U}$. The interested reader is referred to [3] for further details about the definition of the NM.

D. Uncertainty Quantification Issues and Passivisation

In Fig. 4, the results of the ETFEs, $G_i(\omega)$, expressed in Eq. (11), are shown in the complex plane (Nyquist plot), using coloured-dotted lines. It is important to note that, even before approaching an analysis of the results, in an ideal situation the LHP of Fig. 4 should be completely clear. To highlight potential passivity issues obtained in the application of standard uncertainty quantification approaches, it can be noted that, for instance, $G_1(\omega)$, denoted using dotted-blue line in Fig. 4, is partially contained in the LHP. Similarly, the NM $G_o(\omega)$, denoted in Fig. 4 with a deep-grey-solid line, is also partially contained in the LHP. Analogously, the uncertainty set $\mathcal{U}$, denoted in Fig. 4 using grey circles, is partially contained in the LHP. Note that, in Fig. 4, the uncertainty set is shown considering the frequency set required to spectrally

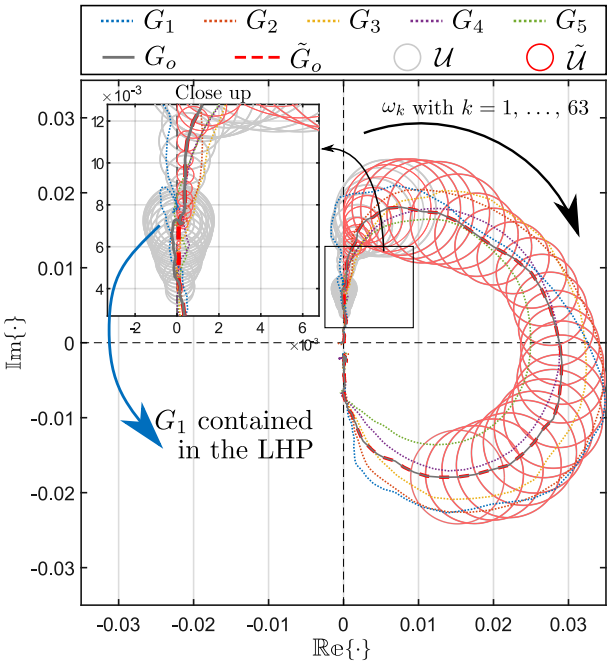

Fig. 4. Nyquist plot of the ETFEs, the NM, its corresponding uncertainty set, passivated NM, and its corresponding passivated uncertainty set.

describe $f_{ex}(t)$, as discussed in Section V-B. Then, in Fig. 4, following the passivisation methodology described in Section IV, the rectified NM, $\tilde{G}_o(\omega)$, and uncertainty set, $\tilde{\mathcal{U}}$, are shown using a dashed-red line and red-circles, respectively, both fully contained in the RHP.

E. Performance Results

To asses the performance of the presented passivisation method, the results presented in [3] are primarily considered as a benchmark. In [3], a similar experimental setup has been considered. However, in the light of the limitations described in Section V-D, the solution presented in [3] proposes to avoid those spectral components that do not guarantee the passivity condition for the complete family of models. In contrast, in this study, by means of the presented passivisation methodology, those components are considered. Thus, considering the WCP, three assessment scenarios are proposed. **Scenario 1:** $G_o(\omega)$ and $\mathcal{U}$, are considered. A nominal, $\hat{\mathbf{u}}_\mathbf{0}^\star$, and, considering circular boundaries, robust $\hat{\mathbf{u}}_\mathbf{r}^\star$ control inputs are computed; **Scenario 2:** $\tilde{G}_o(\omega)$ and $\tilde{\mathcal{U}}$ are considered. A nominal, $\hat{\mathbf{u}}_\mathbf{0}^\star$, and, considering circular boundaries, robust $\hat{\mathbf{u}}_\mathbf{r}^\star$ control inputs are computed; **Scenario 3:** Each ETFE, $G_i(\omega)$, is considered. Using the nominal $\hat{\mathbf{u}}_\mathbf{0}^\star$, and the robust $\hat{\mathbf{u}}_\mathbf{r}^\star$ control inputs computed for **Scenario 2**, the resulting performance is assessed. In each scenario, each control input is applied to the complete considered family of models.

In Fig. 5, using the WCP, the assessment results for Scenarios 1, 2, and 3 are shown, where the results obtained

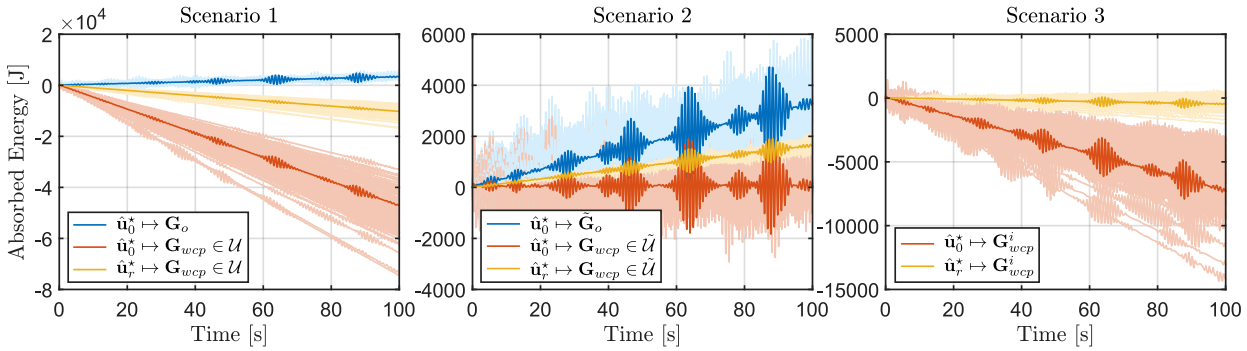

Fig. 5. Performance assessment results for the considered scenarios.

using the synthetically generated wave excitation forces are depicted using light-coloured lines, while the obtained results using the CFD-based wave excitation force is depicted using deep-coloured lines. In Fig. 5, the model that produces the WCP, within the corresponding family of models, is indicated as $\mathbf{G}_{wcp}$. Due to the non-passive conditions in Scenario 1, which represents the results of applying the spectral control methods even under non-passive conditions, the resulting absorbed energy is negative. This negative performance results as a consequence of the violation of the required passivity conditions, due to the use of the NM $G_o(\omega)$ and the uncertainty set $\mathcal{U}$. When the passivisation approach is applied in the second scenario, the absorbed energy is positive in the WCP case. In Scenario 3, which employs the presented passivisation strategy, the absorbed energy, in practical terms, is zero, while with the application of the nominal approach the absorbed energy is negative. Thus, in a realistic scenario, the WCP will be contained between the results shown for Scenarios 2 and 3. Then, using the presented passivisation methodology in a realistic scenario, i.e. not necessarily the WCP, the absorbed energy will be greater than zero. Within this context, it is important to take into account that, in [3], where the invalid (i.e. non-passive) frequency components have been omitted, absorbed energy of the order of 3 J over 100 s is achieved. From a simple comparison between the results in [3] and those presented here, it is straightforward to note that the inclusion of the extra passivised spectral components significantly extends the available energy for power production, while the risk of generating negative power values is virtually reduced to zero.

VI. Conclusion

In this study, a passivisation strategy for energy maximising control for WEC systems is presented. This strategy is essentially based on *a-priori* knowledge of the system, primarily the natural passivity of WEC systems and existing spectral control strategies. The results obtained in the case study show that by using the presented methodology, in comparison with available results in the literature, the absorbed energy can be significantly extended.

Acknowledgement

This material is based upon works supported by Maynooth University via a John and Pat Hume Doctoral (WISH) for Mahdiyeh Farajvand and Science Foundation Ireland (SFI) for funding John V. Ringwood and Valerio Grazioso under contract number 13/IA/1886, and the MaREI (SFI Research Centre for Energy, Climate and Marine). Demián García-Violini is supported by Universidad Nacional de Quilmes.

References

[1] D. Garcia-Violini and J. V. Ringwood, "Energy maximising robust control for spectral and pseudospectral methods with application to wave energy systems," *International Journal of Control*, vol. 94, no. 4, pp. 1102–1113, 2021.

[2] N. Faedo, D. García-Violini, G. Scarciotti, A. Astolfi, and J. V. Ringwood, "Robust moment-based energy-maximising optimal control of wave energy converters," in *2019 IEEE 58th Conf. on Decision and Control (CDC)*. IEEE, 2019, pp. 4286–4291.

[3] M. Farajvand, D. García-Violini, C. Windt, V. Grazioso, and J. V. Ringwood, "Quantifying hydrodynamic model uncertainty for robust control of wave energy devices," in *14th European Wave and Tidal Energy Conference-EWTEC*, 2021.

[4] W. Wang, M. Wu, J. Palm, and C. Eskilsson, "Estimation of numerical uncertainty in computational fluid dynamics simulations of a passively controlled wave energy converter," *Proc. IMechE*, vol. 232, no. 1, pp. 71–84, 2018.

[5] Y. Lao and J. T. Scruggs, "Robust control of wave energy converters using unstructured uncertainty," in *2020 American Control Conference (ACC)*. IEEE, 2020, pp. 4237–4244.

[6] J. V. Ringwood, A. Mérigaud, N. Faedo, and F. Fusco, "An analytical and numerical sensitivity and robustness analysis of wave energy control systems," *IEEE Transactions on Control Systems Technology*, vol. 28, no. 4, pp. 1337–1348, 2019.

[7] C. Windt, N. Faedo, M. Penalba, F. Dias, and J. V. Ringwood, "Reactive control of wave energy devices–the modelling paradox," *Applied Ocean Research*, vol. 109, p. 102574, 2021.

[8] W. E. Cummins, "The impulse response function and ship motions," *Schiffstechnik*, vol. 47, pp. 101–109, 1962.

[9] J. Falnes, *Ocean waves and oscillating systems: linear interactions including wave-energy extraction*. Cambridge Univ. Press, 2002.

[10] G. Bacelli and J. V. Ringwood, "Numerical optimal control of wave energy converters," *IEEE Transactions on Sustainable Energy*, vol. 6, no. 2, pp. 294–302, 2015.

[11] H. K. Khalil, *Noninear Systems*. Prentice-Hall, New Jersey, 1996.

[12] H. G. Weller, G. Tabor, H. Jasak, and C. Fureby, "A tensorial approach to computational continuum mechanics using object-oriented techniques," *Computers in Physics*, vol. 12, no. 6, pp. 620–631, 1998.